The Canadian Mineralogist
Vol. 57, pp. 467-474 (2019)
DOI: 10.3749/canmin.1900011

HUENITE, $Cu_4Mo_3O_{12}(OH)_2$, A NEW COPPER-MOLYBDENUM OXY-HYDROXIDE MINERAL FROM THE SAN SAMUEL MINE, CARRERA PINTO, CACHIYUYO DE LLAMPOS DISTRICT, COPIAPÓ PROVINCE, ATACAMA REGION, CHILE

PIETRO VIGNOLA

CNR-Istituto per la dinamica dei processi ambientali, via Mario Bianco 9, I-20131 Milano, Italia

NICOLA ROTIROTI, G. DIEGO GATTA, AND ANDREA RISPLENDENTE

Dipartimento di Scienze della Terra, Università degli Studi di Milano, via Botticelli 2, I-20133 Milano, Italia

FRÉDÉRIC HATERT

Laboratoire de Minéralogie, Département de Géologie, Université de Liège, Bâtiment B18, Sart Tilman, B-4000 Liège, Belgique

DANILO BERSANI

Dipartimento di Fisica e Scienze della Terra, Università di Parma, Viale G.P. Usberti 7/a, 43124 Parma, Italia

VITTORIO MATTIOLI

Via Keplero 5, I-20124 Milano, Italia

ABSTRACT

Huenite, $Cu_4Mo_3O_{12}(OH)_2$, is a new copper and molybdenum oxy-hydroxide mineral found in the San Samuel Mine, Carrera Pinto, Cachiyuyo de Llampos district, Copiapó Province, Atacama Region, Chile. This new species forms flattened orthorhombic prisms up to 60–70 μm in size, weakly elongated along [001]. Huenite crystals were found on fractured surfaces of a quartz breccia, forming aggregates 1 mm in diameter in close association with lindgrenite, gypsum, dark grayish-brown tourmaline, and an unknown pale purple phase. The color is very dark reddish-brown, with a strong vitreous to adamantine luster. Its streak is pale reddish-brown to pinkish. The mineral is brittle with an irregular fracture and a Mohs hardness of 3.5–4 with a good cleavage on {010}. Its calculated density is 5.1 g/cm^3. The calculated refractive index is 2.18. Huenite is non-fluorescent under 254 nm (short wave) and 366 nm (long wave) ultraviolet light. The empirical formula, calculated on the basis of 3 (Mo+S+Si) atoms per formula unit, is $(Cu_{3.519}Fe^{2+}_{0.403})_{\Sigma 3.922}(Mo_{2.907}S_{0.090}Si_{0.003})_{\Sigma 3.000}O_{12}\cdot(OH)_{2.229}$, with H_2O content calculated for a total of 100 wt.%. Huenite is trigonal, with space group $P3_1/c$ and unit-cell parameters $a = 7.653(5)$ Å, $c = 9.411(6)$ Å, and $V = 477.4(5)$ Å^3 for $Z = 2$. The eight strongest measured powder X-ray diffraction lines are: [d in Å, (I/I_0), (hkl)]: 2.974 (100) (112), 1.712 (59.8) (132), 3.810 (50.6) (110), 2.702 (41.2) (022), 2.497 (38.1) (120), 1.450 (37.2) (134), 6.786 (24.9) (010), and 5.374 (24.5) (011). The mineral, which has been approved by the CNMNC under number IMA 2015-122, is named in honor of Edgar Huen.

Keywords: huenite, new mineral species, copper-molybdenum oxy-hydroxide, San Samuel mine, Chile.

§ *Corresponding author e-mail address*: pietro.vignola@idpa.cnr.it, pietroevignola@gmail.com

Introduction

The San Samuel mine, located in the Atacama region (Chile), is famous for producing high-quality specimens of lindgrenite, a copper molybdate. Its mineral association is characterized by several secondary Bi-, Pb-, and Cu-bearing species belonging to the sulfate and phosphate classes and formed by the oxidation of Bi-Mo-Cu minerals (*i.e.*, powellite, wulfenite, lindgrenite, cornetite, turquoise, pseudomalachite, libethenite). This paper describes the mineralogical features of huenite, a copper-molybdenum oxyhydroxide, occurring in close association with lindgrenite and a mineral belonging to the tourmaline group.

The mineral and its name have been approved by the IMA Commission on New Minerals, Nomenclature and Classification (IMA2015-122, Vignola *et al.* 2016). The mineral is named in honor of Edgar Huen, born in Milano, Italy on May 27th, 1947. Edgar Huen is a senior mineral collector and an expert in Alpine fissure minerals and worldwide systematic mineralogy.

Occurrence, General Appearance, and Physical Properties

Huenite was found by one of the authors (V.M.) and Edgar Huen on lindgrenite specimens from the San Samuel Mine, Carrera Pinto, Cachiyuyo de Llampos district, Copiapó Province, Atacama Region, Chile (27°,4′,40″S and 70°,0′,10″W). Huenite and lindgrenite are oxidation products of primary Cu-sulfide minerals in a body of brecciated quartz porphyry enriched in molybdenite and Cu-sulfides (mainly djurleite, Clark & Sillitoe 1970a, 1970b). These tourmalinized collapse breccia pipes formed under post-magmatic conditions during the Tertiary magmatic cycle and were mineralized by late-stage hydrothermal fluids as open-space fillings. The porphyry bodies have been prospected and mined for copper, gold, and tungsten (Sillitoe & Sawkins 1971).

Huenite occurs as small crystals (60–70 μm long) perched on the surfaces of brittle fractures in the quartz breccia (Fig. 1). The crystals occur as flattened, stout, orthorhombic prisms elongated along [001]. Huenite occurs in close association with lindgrenite, gypsum, and an unidentified pale purple phase. The color is dark reddish-brown, with a strong vitreous to adamantine luster. Its streak is pale reddish-brown to pinkish. The mineral is brittle with an irregular fracture. The Mohs hardness could not be measured due to the small size of the crystals. A good cleavage was observed on {010}. The calculated density is 5.1 g/cm^3. The optical properties of huenite could not be completely determined due to the opacity of the mineral, which prevented observation under crossed Nicols; the birefringence was impossible to estimate. In polarized light, a dark brown color was observed, and the refractive index was estimated to be higher than 2. The refractive index, as calculated from the chemical composition and from the density calculated from the structure, is 2.18 (Mandarino 1979). Huenite is non-fluorescent under 254 nm (short wave) and 366 nm (long wave) ultraviolet light.

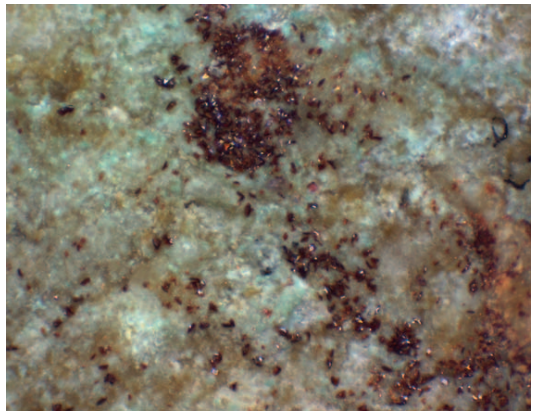

Fig. 1. Crystals of reddish brown huenite; the maximum dimension of the crystals is 60 μm (field of view 1 × 0.75 mm). Type specimen (Collection of Laboratoire de Minéralogie, catalogue number 20399).

Electron Microprobe Analysis

Several small groups of huenite crystals were mounted in epoxy, polished, and carbon coated. Quantitative chemical compositions were obtained from this polished section using a JEOL JXA-8200 electron microprobe working in wavelength-dispersion mode at the Department of Earth Sciences, University of Milano (ESD-MI). The system was operated with an accelerating voltage of 15 kV, a beam current of 5 nA, a spot size of 3 μm, and a counting time of 30 s on the peaks and 10 s on the background. The following minerals were used as standards: omphacite USNM110607 for Na$K\alpha$, orthoclase-PSU OR1A for K$K\alpha$, grossular for Ca$K\alpha$, fayalite 143 for Fe$K\alpha$, realgar for S$K\alpha$ and As$L\alpha$, rhodonite for Zn$K\alpha$ and Mn$K\alpha$, wollastonite for Si$K\alpha$, and apatite A139 for P$K\alpha$. Pure metals (99.99 wt.%) were used as standards for Cu$K\alpha$ and Mo$L\alpha$. The raw data were corrected for matrix effects using the φρZ method in the JEOL series of programs (Pouchou & Pichoir 1991). The following elements were below the detection limit: K, Na, P, As, Zn, Ca, and Mn. Structural and spectroscopic data support the presence of hydroxyl groups, along with the absence of molecular H_2O and CO_2.

TABLE 1. ELECTRON MICROPROBE ANALYSIS OF HUENITE

Constituent	Mean	Range	Stand. Dev.	Probe Standard
wt.%				
MoO_3	55.45	54.70–56.15	0.58	pure Mo metal (99.99 wt.%)
SO_3	0.94	0.87–1.03	0.07	realgar
SiO_2	0.03	0.01–0.05	0.02	wollastonite
CuO	37.08	35.59–39.92	1.66	pure Cu metal (99.99 wt.%)
FeO	3.84	1.93–5.22	1.21	fayalite
H_2O*	2.39			
Total	99.73			

Notes: K, Na, P, As, Zn, Ca, and Mn were below detection limit. * H_2O was calculated for stoichiometry

The averaged electron microprobe composition (five spots) of huenite is reported in Table 1. The empirical formula, calculated on the basis of 3 (Mo+S+Si) atoms per formula unit, is $(Cu_{3.519}Fe^{2+}_{0.403})_{\Sigma 3.922}(Mo_{2.907}S_{0.090}Si_{0.003})_{\Sigma 3.000}O_{12}(OH)_{2.229}$. The simplified formula is $Cu_4Mo_3O_{12}(OH)_2$, which theoretically requires MoO_3 56.23 wt.%, CuO 41.43 wt.%, and H_2O 2.35 wt.%, for a total of 100.00 wt.%.

Powder X-ray Diffraction

The X-ray powder diffraction pattern of huenite was collected with a four-circle Xcalibur diffractometer equipped with a CCD camera, using Debye-Sherrer geometry, at the ESD-MI. Operating conditions were 50 kV, 35 nA, and a sample-to-detector distance of 80 mm. A small volume of specimen was mounted on a glass fiber (50 μm diameter) using a silicone grease. Diffraction data were collected using five frames with a collecting time of 100 s/frame. Least-squares refinement of the unit-cell parameters was performed using the program CELREF 3 (Laugier & Bochu 1999) with starting values from the single-crystal X-ray diffraction experiment (see below). The reflection conditions were found to be consistent with the space group $P3_1/c$ obtained by single-crystal study. The refined unit-cell parameters are $a = 7.65(3)$ Å, $c = 9.428(4)$ Å, and $V = 478(2)$ Å^3. The eight strongest powder X-ray diffraction lines are [d in Å, (I/I_0), (hkl)]: 2.974 (100) (112), 1.712 (59.8) (123), 3.810 (50.6) (110), 2.702 (41.2) (022), 2.497 (38.1) (120), 1.450 (37.2) (134), 6.786 (24.9) (010), and 5.374 (24.5) (011). The complete list of indexed reflections is reported in Table 2.

TABLE 2. X-RAY POWDER DIFFRACTION DATA FOR HUENITE (d in Å)

I/I_0	d_{obs}	d_{calc}	h k l
24.9	**6.786**	**6.624**	1 0 0
24.5	**5.372**	**5.420**	1 0 $\bar{1}$
50.6	**3.810**	**3.825**	**1 1 0**
9.2	3.287	3.312	2 0 0
100	**2.974**	**2.970**	**1 1 2**
41.2	**2.702**	**2.710**	**2 0 2**
38.1	**2.497**	**2.504**	**2 1 0**
23.7	**2.203**	**2.208**	3 0 0
19.9	1.960	1.958	2 1 3
7.1	1.823	1.814	1 0 5
59.8	**1.712**	**1.712**	**3 1 2**
4	1.619	1.611	3 0 4
4.4	1.554	1.563	4 0 2
12.6	1.505	1.506	2 1 5
37.2	**1.450**	**1.449**	**3 1 4**
6.5	1.374	1.368	3 2 3
5.7	1.326	1.325	5 0 0
12.3	1.182	1.183	3 2 5
6.4	1.042	1.042	6 0 3
6	0.989	0.989	4 3 4
4.6	0.945	0.945	4 3 5
3.9	0.912	0.913	4 1 8
7.6	0.879	0.879	5 2 6

Single-Crystal X-ray Diffraction

Single-crystal X-ray diffraction data were collected at the ID09 beamline of the European Synchrotron Radiation Facility (ESRF) using the experimental setup described by Merlini & Hanfland (2013). Further details pertaining to the data collection are reported in Table 3. Bragg peaks were then indexed, and their intensities integrated and corrected for Lorentz-polarization effects using the CrysAlis package (Agilent 2012). The lattice of the huenite structure is hexagonal, with $a = 7.653(5)$ Å, $c = 9.411(6)$ Å, and $V = 477.4(5)$ Å^3, and the reflection conditions are consistent with space group $P3_1/c$.

The crystal structure of huenite was solved using the SUPERFLIP program (based on the charge flipping algorithm, Palatinus & Chapuis 2007) implemented in JANA2006 (Petricek *et al*. 2014), on the basis of the intensity data (Table 3). One *Mo* site, two independent *Cu* sites, six independent *O* sites, and two independent *H* sites were located (Table 4). The anisotropic structural refinement was performed using the JANA software (Petricek *et al*. 2014). Neutral atomic scattering factors of Cu, Mo, and O were used. The structure refinement indicated full occupancy of the *Mo* and *Cu*(1) sites whereas the *Cu*(2) site showed a partial occupancy (Table 4). When convergence was achieved the residuals ranged between +1.12 and –1.25 e^-/Å^3. The final $R1(F)$ value was 0.031 for 704 unique reflections with $F_o > 4\sigma(F_o)$ and 69 refined parameters (Table 3). Anisotropic displacement pa-

TABLE 3. DETAILS OF THE DATA COLLECTION AND STRUCTURE REFINEMENT OF HUENITE

Crystal shape	Irregular prism
Crystal size (mm)	60 × 40 × 20
Crystal color	Reddish-brown, translucent
T (K)	298
Unit-cell constants	*a* = 7.653 (5) Å *c* = 9.411 (6) Å *V* = 477.4(5) Å^3
Reference chemical formula	$Cu_4Mo_3O_{12}(OH)_2$
Space Group	$P3_1/c$
Z	2
Radiation type	Synchrotron light source
Wavelength (Å)	0.4134
Diffractometer	ID09A beamline
Data-collection method	ω scan
Step size (°)	1
Max. *q* (°)	32.42
h_{min}, h_{max}	–7, +11
k_{min}, k_{max}	–11, +11
l_{min}, l_{max}	–13, 8
No. measured reflections	1235
No. unique reflections	747
No. unique refl. with $F_o > 4\sigma(F_o)$	704
No. refined parameters	69
Refinement on	*F*
*R*1 (*F*) with $F_o > 4\sigma(F_o)$	0.031
*R*1 (*F*) for all the unique reflections	0.034
*wR*2 (F^2)	0.036
Residuals (e$^-$/Å^3)	+1.12/–1.25

Note: Rint = $\sum|F^2obs–F^2obs(mean)|/\sum(F^2obs)$; *R*1 = $\sum(|Fobs–Fcalc|)/\sum|Fobs|$; *wR*2 = $(\sum(w(F^2obs–F^2calc)_2)/\sum(w(F^2obs)_2)0.5$, $w = 1/(\sigma^2(Fobs)+0.0001F^2obs)$.

rameters and selected bond-distances are given in Tables 5 and 6, respectively.

Huenite is a copper molybdenum oxy-hydroxide mineral with endmember chemical formula $Cu_4Mo_3O_{12}(OH)_2$. Two views of the crystal structure of huenite are shown in Figure 2. The structure of huenite consists of clusters of $Mo_3O_{12}(OH)$ and $Cu_4O_{16}(OH)_2$ units (Figs. 2 and 3). Three edge-sharing Mo octahedra form the $Mo_3O_{12}(OH)$ unit, whereas four edge-sharing Cu-octahedra form the $Cu_4O_{16}(OH)_2$ units (with a "U" shape), which are in turn share edges to form a sheet of Cu octahedra parallel to (001) (Figs. 2 and 3). The $MoO_5(OH)$ octahedron shows a difference between the longest and the shortest bond distance of about 0.56 Å, followed by the $CuO_5(OH)$ polyhedron with $\Delta(Cu(1)–O)_{max} \sim 0.49$; the remaining Cu_2O_6 polyhedron is the most regular, with $\Delta(Cu(2)–O)_{max} \sim 0.03$ (Table 6). The geometry of the OH groups and the hydrogen bonding scheme is well-resolved from the refinement of the crystal structure. The *H*(1)–*O*(5) and *H*(2)–*O*(6) distances are 0.90 and 0.97 Å, respectively (Table 7), and there are two three-forked hydrogen bonds: *H*(1)···*O*(3) and *H*(2)···*O*(4) with bond lengths of 2.39 and 2.28 Å, respectively, and *O*(5)–*H*(1)···*O*(3) and *O*(6)–*H*(2)···*O*(4) angles of 133.8° and 133.0°. (Table 7, Fig. 4A). The latter are virtual since we used an average special position for the two H atoms instead of a general one. As a consequence, the atomic displacement parameters of these atoms were fixed to a common value of 0.06 Å^2. Likely, the true position of the H atoms is disordered in the (001) plane, perpendicular to the *O*(5)–*H*(1) and *O*(6)–*H*(2) bonds. In this configuration the D–H···A angles approach the correct value of 180° (Fig. 4B). The *Cu*(2) site is partially occupied, as shown by the structure refinement (Table 4). Therefore, its occupancy from the structure refinement is 24.4 e$^-$, in fairly good agreement with the microprobe results which indicate an occupancy of 27.3 e$^-$. The bond-valence calculation

TABLE 4. REFINED POSITIONAL AND THERMAL DISPLACEMENT PARAMETERS (Å^2) OF HUENITE AT 298 K

Atom	Occ	*x*	*y*	*z*	U_{iso}/U_{eq}
Cu(1)	Cu 1	0.7604(2)	0.0005(2)	–0.1899(5)	0.0139(4)
Cu(2)	Cu 0.84(1)	2/3	1/3	0.3219(5)	0.0172(8)
Mo	Mo 1	0.4359(1)	0.0477(1)	0.0557(5)	0.0073(2)
O(1)	1	0.5260(10)	–0.0756(10)	–0.0681(10)	0.017(3)
O(2)	1	0.4490(9)	0.2841(10)	0.1688(10)	0.014(3)
O(3)	1	0.2469(9)	0.0508(10)	–0.0535(11)	0.016(3)
O(4)	1	0.3055(10)	–0.1315(10)	0.1794(9)	0.016(3)
O(5)	1	0	0	–0.2820(16)	0.015(4)
O(6)	1	2/3	1/3	–0.0526(17)	0.018(4)
H(1)	1	0	0	–0.378(12)	0.06(7)
H(2)	1	2/3	1/3	–0.153(12)	0.06(7)

TABLE 5. ANISOTROPIC THERMAL DISPLACEMENT PARAMETERS (Å^2) OF HUENITE

	U^{11}	U^{22}	U^{33}	U^{12}	U^{13}	U^{23}
Cu(1)	0.0117(4)	0.0177(4)	0.0110(6)	0.0063(4)	–0.0008(4)	0.0040(4)
Cu(2)	0.0222(10)	0.0222(10)	0.0073(15)	0.0111(5)	0	0
Mo(1)	0.0082(3)	0.0076(3)	0.0052(3)	0.0033(2)	0.0006(2)	0.0001(3)
*O*1	0.019(3)	0.016(3)	0.019(5)	0.011(3)	0.004(3)	0.003(3)
*O*2	0.021(3)	0.010(3)	0.011(4)	0.008(2)	0.005(3)	–0.001(2)
*O*3	0.017(3)	0.010(3)	0.022(5)	0.007(2)	–0.001(3)	–0.002(3)
*O*4	0.017(3)	0.019(3)	0.014(4)	0.011(3)	0.003(3)	0.002(3)
*O*5	0.013(3)	0.013(3)	0.019(8)	0.007(2)	0	0
*O*6	0.020(4)	0.020(4)	0.012(8)	0.010(27)	0	0

TABLE 6. SELECTED BOND DISTANCES (Å) FOR HUENITE

Cu(1)–O3	1.953(9)	*Cu*(2)–O1	×3	2.057(7)	*Mo*(1)–O4	1.692(8)
Cu(1)–O1	1.957(9)	*Cu*(2)–O2	×3	2.089(8)	*Mo*(1)–O3	1.784(9)
Cu(1)–O2	1.978(8)	<***Cu2–O***>		**2.073**	*Mo*(1)–O1	1.836(10)
Cu(1)–O5	2.030(7)				*Mo*(1)–O2	2.058(9)
Cu(1)–O4	2.391(8)				*Mo*(1)–O2′	2.146(8)
Cu(1)–O3′	2.443(10)				*Mo*(1)–O6	2.253(8)
<***Cu*(1)–O**>	**2.125**				<***Mo*(1)–O**>	**1.962**

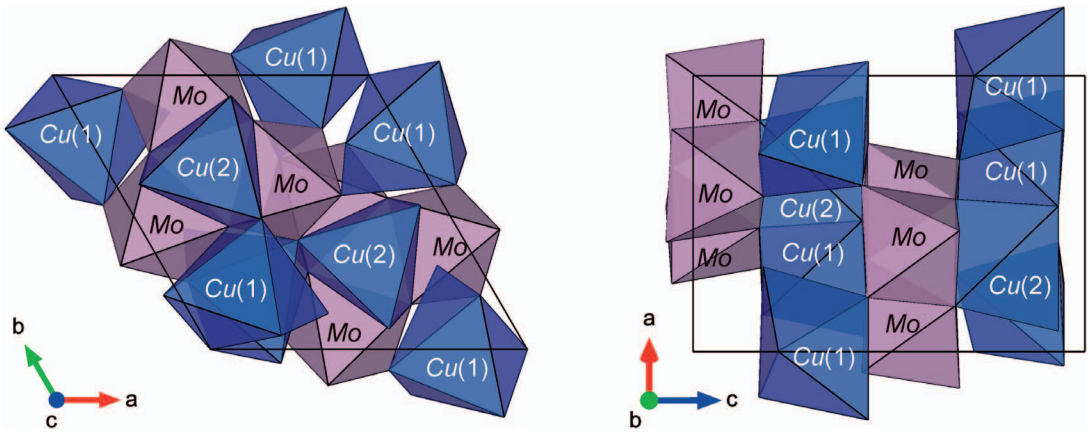

FIG. 2. Two views of the crystal structure of huenite (blue = Cu, purple = Mo): (left side) down [001] and *(right side)* down [100].

TABLE 7. HYDROGEN-BOND GEOMETRY IN HUENITE (Å, °)

D–H···A		D–H distance	H···A distance	D–A distance	A–H···D angle
O5–H1···O3	×3	0.91(11)	2.39(8)	3.085(16)	134(2)
O6–H2···O4	×3	0.95(11)	2.29(8)	3.020(16)	134(3)

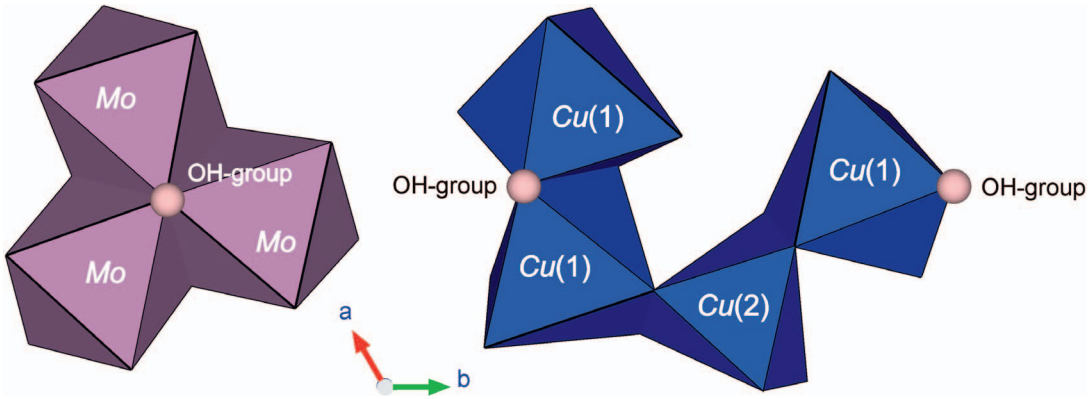

FIG. 3. (Left side) Configuration of the $Mo_3O_{12}(OH)$ unit. (Right side) Configuration of the $Cu_4O_{16}(OH)_2$ unit. (blue = Cu, purple = Mo; white = H).

(Table 8) shows a very good charge balance for all different crystallographic sites, evidencing a very good agreement between the microprobe analysis and crystal structure refinement.

On the basis of its crystal structure, huenite could be classified as an "Oxi-hydroxide, without H_2O; sheets of edge-sharing octahedra" following the Strunz classification (4.FE) (Strunz and Nickel 2001). In the Dana classification, huenite belongs to class 6.2: hydroxides and oxides containing hydroxyl $X(OH)_2$.

RAMAN SPECTROSCOPY

Raman spectra were collected from single crystals using an Olympus BX40 microscope attached to a Jobin-Yvon Horiba LabRam confocal Raman spectrometer, equipped with a charge-coupled detector (CCD), at the University of Parma. The spectra were collected by exciting the sample with 473.1 nm laser light. The laser beam was focused on the sample with a spot-size of ~2 μm diameter (objective 50×) and the confocal aperture was set at 150 μm. The Raman spectra were collected in backscattered geometry, in the range 100–4000 cm^{-1}, with 60 s counting time and four accumulations (Figs. 5 and 6). Figure 5 shows three Raman spectra collected with three different (randomly selected) crystal orientations.

The Raman spectrum of huenite is strongly dependent on the crystallographic orientation of the crystal; as shown in Figure 5, the intensity of the peaks between 800 and 900 cm^{-1} is highly sensitive to the orientation of the laser beam with respect to the crystal axes. A list of the observed Raman bands is given in Table 9. The presence of two independent hydroxyl groups in the structure is corroborated by the almost overlapped Raman active bands at about 3430 cm^{-1},

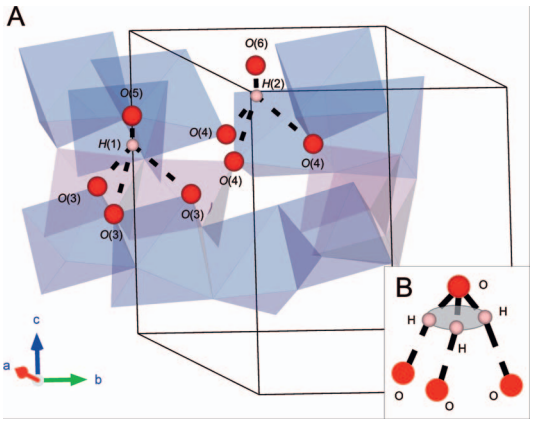

FIG. 4. (A) Hydrogen bonding scheme in huenite with H1 and H2 at special positions; (B) the inset shows the real configuration of the hydrogen bond style. (blue = Cu, purple = Mo; white = H)

TABLE 8. BOND-VALENCE CALCULATION FOR HUENITE

	Cu(1)	Cu(2)*	Mo	H(1)	H(2)	sum
O1	0.467	0.351(x3)	1.212			2.030
O2	0.441	0.321(x3)	0.641			1.901
			0.498			
O3	0.473		1.406			1.998
	0.119					
O4	0.138		1.83			1.968
O5	0.381			1.019		2.162
O6			0.367		0.928	2.029
sum	2.019	2.016	5.954			

After Gagné & Hawthorne (2015); * calculated according to chemistry.

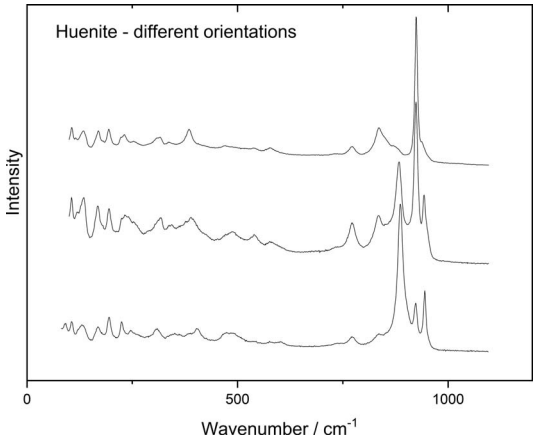

FIG. 5. Raman spectra of huenite with three different (randomly selected) crystal orientations (wavelength 473 nm, range: 200–1100 cm^{-1}).

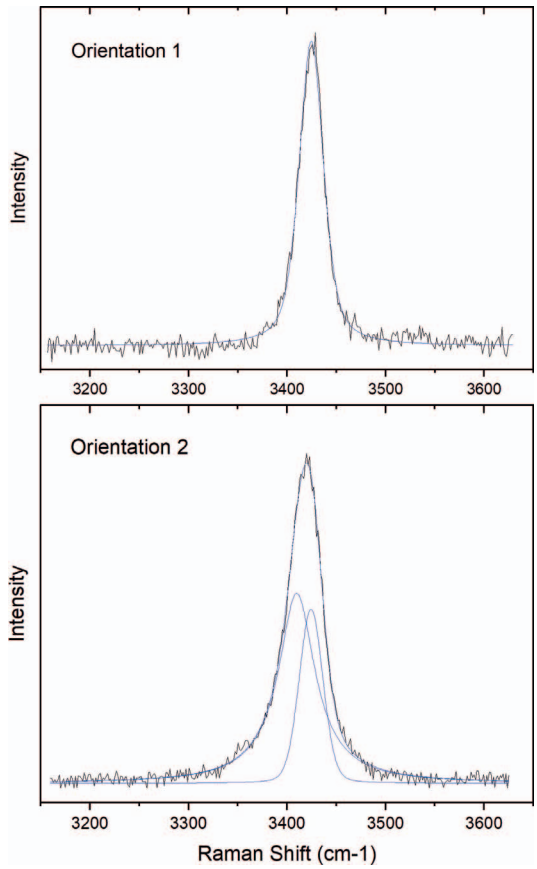

FIG. 6. Raman spectra of huenite at high frequency (range: 3100–3700 cm^{-1}) showing stretching modes of the hydroxyl groups (wavelength 473 nm).

TABLE 9. RAMAN BANDS OF HUENITE

Wavenumber (cm^{-1})	Intensity	Wavenumber (cm^{-1})	Intensity
105	m	488	m
116	w	499	vw (sh)
122	sh	541	w
134	m	580	w
168	m	601	vw
180	vw	690	vw (sh)
195	m	734	w
224	w	772	m
232	m	835	s
242	w	853	sh
254	w	870	sh
290	vw	883	vs
311	m	917	sh
318	m	923	vs
340	w	942	s
365	sh	949	sh
391	m		
422	m	3424	s
470	m	3410	s

Notes: * vw = very weak, v = weak, m = medium, s = strong, vs = very strong, sh = shoulder.

ascribable to the stretching modes of the hydroxyl groups (Fig. 6). The Raman spectrum of huenite in the range of the stretching modes of the hydroxyl groups (Fig. 6) depends on the orientation of the crystals, as seen in the low wavenumbers range. A single sharp band at 3424 cm^{-1} (width 29 cm^{-1}) is visible in some orientations (orientation 1 in Fig. 6), while in some other orientations (orientation 2 in Fig. 6) the Raman band seems to down-shift and broaden. The most probable explanation is illustrated by deconvolution of the band into two smaller bands. A first band, identical to the one visible in orientation 1 (center = 3424 cm^{-1}, width = 29 cm^{-1}) is accompanied by a second band, arising only in particular orientations, with center at 3410 cm^{-1} and width 48 cm^{-1}. This can be explained by the presence of two independent hydroxyl groups in the structure. At lower wavenumbers, a series of strong peaks due to Mo–O stretching motion is visible between 945 and 470 cm^{-1}, with the wavenumber of the peaks roughly decreasing as the Mo–O bond length increases. The large number of peaks reflects the presence of non-perfectly equivalent Mo–O6 octahedra and their strong distortion. At wavenumbers between 190 and 380 cm^{-1}, the Raman peaks are attributed to O–M–O bending vibrations (with M = Mo, Cu). At lower wavenumbers, bands involving the motions of MO_6 octahedra are expected (Dieterle *et al*. 2002, Seguin *et al*. 1995, Debbichi *et al*. 2012).

Acknowledgments

The authors are grateful to Marco Merlini for the single-crystal X-ray data collection at ESRF (Grenoble). The Authors are grateful to Associate Editor Aaron Lussier and to reviewers Ferdinando Bosi and Adam Pieczka for their valuable suggestions.

References

Agilent (2012) *Xcalibur CCD system*, CrysAlis Software system. Agilent Technologies, XRD Products. Yarnton, United Kingdom.

Clark, A.H. & Sillitoe, R.H. (1970a) Tungstenian wulfenites, Mina San Samuel, Cachiyuyo De Llampos, Chile. *American Mineralogist* **55**, 2114–2118.

Clark, A.H. & Sillitoe, R.H. (1970b) Cuprian sphalerite and a probable copper-zinc sulfide, Cachiyuyo De Llampos, Copiapo, Chile. *American Mineralogist* **55**, 1021–1025.

Debbichi, L., Marco de Lucas, M.C., Pierson, J.F., & Krügerdx, P. (2012) Vibrational Properties of CuO and Cu_4O_3 from First-Principles Calculations, and Raman and Infrared Spectroscopy. *Journal of Physical Chemistry* **116**, 10232–10237.

Dieterle, M., Weinberg, G., & Mestl, G. (2002) Raman spectroscopy of molybdenum oxides Part I. *Physical Chemistry Chemical Physics* **4**, 812–821.

Gagné, O.C. & Hawthorne, F.C. (2015) Comprehensive derivation of bond-valence parameters for ion pairs involving oxygen. *Acta Crystallographica* **B71**, 562–578.

Laugier, J. & Bochu, B. (1999) *CELREF*: Cell parameters refinement program from powder diffraction diagram. Laboratoire des Matériaux et du Génie Physique, EcoleNationaleSupérieur de Physique de Grenoble (INGP), Grenoble, France

Mandarino, J.A. (1979) The Gladstone-Dale relationship. Part III: some general applications. *Canadian Mineralogist* **17**, 71–76.

Merlini, M. & Hanfland, M. (2013) Single-crystal diffraction at megabar conditions by synchrotron radiation. *High Pressure Research* **33**, 511–522.

Palatinus, L. & Chapuis, B. (2007) *SUPERFLIP* – a computer program for the solution of crystal structures by charge flipping in arbitrary dimensions. *Journal of Applied Crystallography* **40**, 786–790.

Petricek, V., Dusek, M., & Palatinus, L. (2014) Crystallographic Computing System JANA2006: General Features. *Zeitschrift für Kristallographie* **229**, 345–352.

Pouchou, J.L. & Pichoir, F. (1991) Quantitative analysis of homogeneous or stratified microvolumes applying the model PAP. *In* Electron Microprobe Quantitation (K.F.J. Heinrich & D.E. Newbury, eds.). Plenum Press, New York, United States (31–76).

Seguin, L., Figlarz, M., Cavagnat, R., & Lassegues, J.C. (1995) Infrared and Raman spectra of MoO_3 molybdenum trioxides and $MoO_3{\cdot}xH_2O$ molybdenum trioxide hydrates. *Spectrochimica Acta part A: Molecular and Biomolecular Spectroscopy* **51**, 1323–1344.

Sheldrick, G.M. (1997) *SHELX-97* – A program for crystal structure refinement. University of Göttingen, Göttingen, Germany.

Sillitoe, R.H. & Sawkins, F.J. (1971) Geologic, mineralogic and fluid inclusion studies relating to the origin of copper-bearing tourmaline breccia pipes, Chile. *Economic Geology* **66**, 1028–1041.

Strunz, H. & Nickel, E.H. (2001) *Strunz mineralogical tables*. 9th Edition, Schweizerbart, Suttgart, Germany, 870 pp.

Vignola, P., Gatta, G.D., Merlini, M., Rotiroti, N., Hatert, F., Bersani, D., Risplendente, A., Gentile, P., & Pavese, A. (2016) Huenite, IMA 2015-122. CNMNC Newsletter No. 31, June 2016, page 692; *Mineralogical Magazine* **80**, 691–697.

Received February 8, 2019. Revised manuscript accepted May 8, 2019.